

## Variable-Fidelity Response Feature Surrogates for Accelerated Statistical Analysis and Yield Estimation of Compact Microwave Components

Slawomir Koziel<sup>1,2</sup> and Adrian Bekasiewicz<sup>2</sup>

<sup>1</sup> Engineering Optimization & Modeling Center, School of Science and Engineering, Reykjavik University, Menntavegur 1, 101 Reykjavik, Iceland

[koziel@ru.is](mailto:koziel@ru.is)

<sup>2</sup> Faculty of Electronics, Telecommunications and Informatics, Gdansk University of Technology, Narutowicza 11/12, 80-233 Gdansk Poland

[bekasiewicz@ru.is](mailto:bekasiewicz@ru.is)

**Abstract:** Accounting for manufacturing tolerances is an essential part of a reliable microwave design process. Yet, quantification of geometry and/or material parameter uncertainties is challenging at the level of full-wave electromagnetic (EM) simulation models. This is due to inherently high cost of EM analysis and massive simulations necessary to conduct the statistical analysis. In this paper, a low-cost and accurate yield estimation procedure for compact microwave couplers is proposed. Our technique involves variable-fidelity electromagnetic (EM) simulation models, as well as fast surrogates constructed using a response feature approach. In order to improve the computational efficiency of the analysis, the primary surrogate is obtained from the characteristic points of the low-fidelity model and, subsequently, corrected using a single evaluation of the high-fidelity model. Combination of both methods results in an extremely low cost of yield estimation being just a few high-fidelity EM analyses. For the sake of demonstration, a compact hybrid rat-race coupler operating at 1 GHz is considered. Yield estimation is carried out under several scenarios concerning various probability distributions of the geometry parameter deviations. Reliability of the approach is verified by comparing the results with direct Monte Carlo analysis and single-fidelity feature-based yield estimation.

### 1. Introduction

Typical microwave design procedures or optimization methods used therein (e.g., [1], [2]), as well as vast majority of novel topologies of particular components and devices (filters [3], couplers [4], power dividers [5], etc.) aim at producing so-called nominal designs. This means that geometry and material parameters are assumed, upon prototyping, to feature the values they were designed for. Potential deviations due to the fabrication tolerances or other uncertainties (e.g., the lack of knowledge of the actual value of substrate dielectric permittivity) are neglected. Obviously, the tolerances may play a major role in the actual system performance. Consequently, quantification of these effects, both aleatory (or pertinent to manufacturing deviations) and epistemic (e.g., related to limited knowledge of the operating conditions or the computational model utilized to represent the system), is critical from the point of view of adequate assessment of the design robustness. In robust design [6]-[9], as opposed to nominal design, the purpose is not to simply improve the values of given performance figures as much as possible but to maximize the probability of satisfying given design specifications under the assumed distributions of the tolerances. Various techniques have been developed to carry out robust design, under different names and sometimes slightly different objectives (tolerance-aware design, design centering, yield-driven design [10], [11]).

The fundamental component of robust design algorithms is statistical analysis [12]-[15]. The goal of it may be determination of the statistical moments of the system response outputs assuming certain probability distributions of the input parameters (and/or operating conditions) [15]. The objective may also be estimation of the yield, which is

probability of satisfying performance requirements imposed upon the system, again under the assumed manufacturing tolerances and other uncertainties. Conventional methods such as Monte Carlo (MC) analysis become problematic if the structure of interest is evaluated using full-wave electromagnetic (EM) simulation. This is due to the high computational cost of massive EM evaluations necessary. In particular, the Monte Carlo analysis is slowly convergent so that anything between a few hundred to a few thousands of random samples are necessary for reliable yield estimation. A worst-case analysis is a possible workaround [16], however, it normally provides overly pessimistic results. Nowadays, computational speedup is usually achieved by means of surrogate models such as response surface approximation (RSA) one [17], or polynomial chaos expansion [14], [18]. At the same time, the issues related to dimensionality of the parameter space, can be addressed to certain extent by utilizing techniques such as principal component analysis (PCA) [19] or space mapping [20], [21].

Yet another approach, which allows for addressing both the problem of response nonlinearity and design space dimensionality, is utilization of so-called response features [22]. It is applicable in situations where the response of the component of interest has a well-defined structure (e.g., narrow-band or multi-band antennas, microwave filters, etc.). Feature-based statistical analysis of microwave filter has been demonstrated in [22]. The key factor here is that reformulating the surrogate modelling problems in terms of appropriately defined characteristic points permits “smoothing out” the functional landscape of the component response. This results in a significant reduction of the number of training data points necessary to construct the surrogate.

The purpose of this work is to advance the feature-based statistical analysis into a variable-fidelity framework, where the surrogate is primarily constructed using the data from the low-fidelity EM model, subsequently corrected by means of sparsely sampled data from the high-fidelity model. Assuming sufficient correlation between EM simulations of various fidelities (which is normally the case, especially if both models are evaluated using the same solver), the surrogate model is reliable yet established at much lower computational cost as compared to single-fidelity framework. As a result, the yield estimation can be realized considerably faster. For the sake of demonstration, a compact equal split rat-race coupler operating at 1 GHz is considered. The yield estimation is carried out under various scenarios concerning probability distributions of manufacturing tolerances. The computational cost of the process corresponds to only less than three EM simulations of the coupler at high-fidelity level of analysis. At the same time, the accuracy is satisfactory, as confirmed through benchmarking with both direct EM-based Monte Carlo and single-level feature-based analyses. The main original contributions of the work include: (i) incorporation of variable-fidelity EM simulations into the statistical analysis framework resulting in dramatic reduction of the computational cost of the process, (ii) correlation analysis of the low- and high-fidelity model feature point coordinates resulting in the development of the appropriate type of correction technique for the former, and (iii) demonstrating of the proposed concept on the challenging real-world design case study.

## 2. Response Features for Microwave Couplers

In this section, we briefly recall the concept of feature-based analysis, define response features for microwave couplers as well as illustrate the benefits of formulating the statistical analysis problem at the level of feature points rather than original responses (here,  $S$ -parameter characteristics).

### 2.1. Statistical Analysis Using Response Features

Statistical analysis is carried out to account for perturbations of geometry and material parameters due to manufacturing tolerances. These are quantified using the assumed probability distributions, typically Gaussian or uniform. For many types of microwave structures, the system responses are highly nonlinear and therefore difficult to handle even locally (e.g., when constructing auxiliary surrogates). A feature-based framework proposed in [23] suggested reformulating the original design problem with the objective function defined at the level of frequency characteristics ([23] focused on solving optimization tasks) in terms of appropriately defined characteristic points of the system response. This leads to a reduced nonlinearity of the functional landscape under consideration, and, consequently, computational savings. Later, the feature-based approach has been successfully applied to a statistical analysis of microwave filters [22].

### 2.2. Response Features of Microwave Couplers

In this paper, the class of microwave structures of interest are couplers. One of the challenges is the necessity of handling several performance figures such as operating frequency  $f_0$ , bandwidth  $B$  (typically at the  $-20$  dB level for matching and

isolation characteristics), as well as power split (i.e., difference of the transmission responses  $dS = |S_{31}| - |S_{21}|$  at  $f_0$ ). A typical  $S$ -parameter characteristics of a coupler, here optimized for  $f_0 = 1$  GHz, are shown in Fig. 1. The same figure also shows the response features which are defined to permit accounting for the aforementioned design requirements. In practice, the characteristic points are extracted from the original responses through post-processing.

### 2.3. Advantages of Feature-Based Approach

The primary benefits of using response features can be observed by analysing the variability of the original coupler responses ( $S$ -parameters vs. frequency) and the characteristic points as shown in Fig. 2. As indicated in Fig. 2(b), the dependence of the feature point coordinates on the geometry parameters is much smoother and only weakly nonlinear. This enables a possibility of constructing accurate surrogate models using a small number of training samples. At the same time, feature-based models carry sufficient information to account adequately for the performance specifications.

## 3. Yield Estimation by Variable-Fidelity Response Features

In this section, the yield estimation technique using variable-fidelity response features is explained in detail. Section 4 provides a verification case study.

### 3.1. Yield Estimation

The aggregated vector of feature points, i.e., the vector containing both their frequency and level coordinates, will be denoted by  $F_f(\mathbf{x})$ . The essential coupler performance figures—here, the bandwidth  $B(F_f(\mathbf{x}))$  and the power split ratio  $dS(F_f(\mathbf{x}))$ —can be readily extracted from  $F_f(\mathbf{x})$ . The design requirements are imposed through the maximum power split error  $dS_{\max}$  and the minimum accepted bandwidth  $B_{\min}$ . Given these, the estimated yield can be found as

$$Y = N^{-1} \sum_{k=1}^N H(\mathbf{x}^{(k)}) \quad (1)$$

where  $H(\mathbf{x}) = 1$  if  $|dS(F_f(\mathbf{x}))| \leq dS_{\max}$  and  $B(F_f(\mathbf{x})) \geq B_{\min}$ ;  $H(\mathbf{x}) = 0$  otherwise. The set  $\mathbf{x}^{(k)} = \mathbf{x}^{(0)} + \mathbf{d}\mathbf{x}^{(k)}$ ,  $k = 1, \dots, N$ , is a sample set in which  $\mathbf{x}^{(0)}$  stands for a nominal design, whereas  $\mathbf{d}\mathbf{x}^{(k)}$  are random deviations allocated according to the assumed probability distribution.

### 3.2. Response-Feature Surrogates

The primary way of reducing the computational cost of statistical analysis is to perform yield estimation using an auxiliary surrogate model  $s(\mathbf{z})$  constructed at the level of response features, where  $\mathbf{z}$  stands for a vector of perturbations with respect to the nominal design  $\mathbf{x}^{(0)}$ . The model is a second-order polynomial of the form (here,  $[ ]^2$  is understood component-wise)

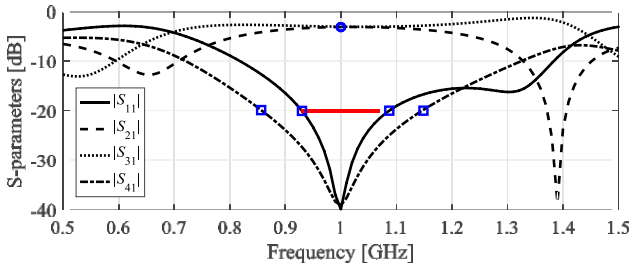


**Fig. 1.** *S*-parameters of a microwave coupler along with response features corresponding to  $-20$  dB bandwidth  $B$ , operating frequency  $f_0$ , and the power split. Here, a symmetric part of the bandwidth is considered as marked using the thick horizontal line. The level features  $L_1$  ( $S_{21}$ ) and  $L_2$  ( $S_{31}$ ) are marked by  $(\circ)$ . Frequency features (from the left)  $B_1$ ,  $B_2$ ,  $B_3$ , and  $B_4$  are marked by  $(\square)$ . Note an overlap between some of the points, which is due to equal power split for the particular design shown here.

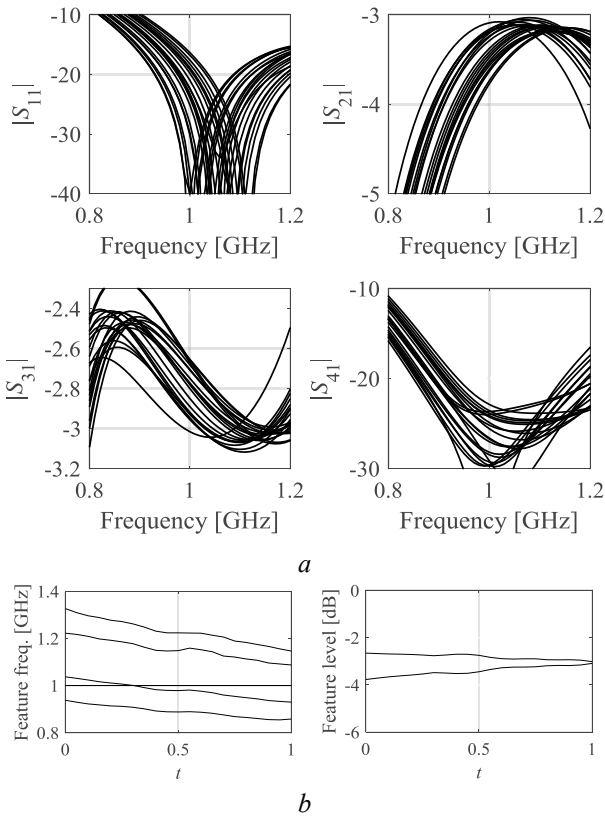


**Fig. 2.** *Variability of the S-parameters and selected response feature point coordinates when evaluating the coupler response along a selected line segment in the design space  $t\mathbf{x}^{(1)} + (1-t)\mathbf{x}^{(2)}$ , parameterized by  $0 \leq t \leq 1$ :*

(a) *S*-parameters,  
(b) selected response features (top: frequency, bottom: level coordinates).

$$\mathbf{s}(\mathbf{z}) = \mathbf{a}_0 + \mathbf{A}_1 \mathbf{F}(\mathbf{x}^{(0)} + \mathbf{z}) + \mathbf{A}_2 \left[ \mathbf{F}(\mathbf{x}^{(0)} + \mathbf{z}) \right]^2 \quad (2)$$

The model coefficient matrix  $\mathbf{A} = [\mathbf{a}_0 \mathbf{A}_1^T \mathbf{A}_2^T]^T$  is obtained by solving the following regression problems

$$\mathbf{s}(\mathbf{x}^{(0)} + \mathbf{x}_B^{(j)}) = \mathbf{F}(\mathbf{x}^{(0)} + \mathbf{x}_B^{(j)}) \quad (3)$$

where  $\mathbf{z} = \mathbf{x}_B^{(j)}$ ,  $j = 0, 1, \dots, N_B$ , are the base designs. Here, a star distribution design of experiments is utilized [24] with

$\mathbf{x}_B^{(0)}$  being a zero vector and  $\mathbf{x}_B^{(j)} = d \cdot \mathbf{e}^{(j)}$  for even  $j$  and  $\mathbf{x}_B^{(j)} = -d \cdot \mathbf{e}^{(j)}$  for odd  $j$ . Here,  $\mathbf{e}^{(j)}$  are the standard  $R^n$  basis vectors of the form  $\mathbf{e}^{(j)} = [0 \dots 0 \ 1 \ 0 \dots 0]^T$  with 1 on the  $j$ th position;  $d$  is the maximum assumed parameter deviation (e.g., 0.05 mm). The rationale behind selecting the particular analytical form of the surrogate (2), i.e., low-order polynomial is twofold: (i) only slightly non-linear dependence of feature point coordinates on geometry parameters of the circuit under analysis (cf. Section 2.2) only requires to account for main variable interactions and curvatures, especially that the analysis is conducted in a small vicinity of the nominal design; (ii) the considered surrogate can be established using a small number of training data samples, here,  $2M + 1$  (with  $M$  being the number of structure parameters) which dramatically reduces the cost of analysis compared to EM-based MC, and well corresponds with the factorial design of experiments strategy (specifically, the mentioned star distribution).

### 3.3. Variable-Fidelity Surrogates

In this paper, in order to achieve an additional speedup, the feature-based surrogate constructed at the level of the high-fidelity EM model is replaced by the corresponding model obtained based on the low-fidelity EM simulation data, denoted as  $\mathbf{F}_c(\mathbf{x})$ . In practice, the low-fidelity model can be made several times faster than the high-fidelity one by reducing discretization density of the structure. Clearly, this leads to a certain loss in accuracy: usually both the frequency and level shifts can be observed between the low- and high-fidelity model responses. Despite these discrepancies, the models are well correlated as illustrated in Fig. 3 for selected (random) pairs of designs.

Before the surrogate model (2) constructed from the low-fidelity feature point vectors can be used for yield estimation, it has to be corrected to account for the model discrepancies. Here, the correction is implemented using a single high-fidelity model evaluation at the nominal design. Consequently, it is of a zero-order type and takes a form of

$$\mathbf{s}(\mathbf{z}) = \mathbf{s}_c(\mathbf{z}) + \left[ \mathbf{F}_f(\mathbf{x}^{(0)}) - \mathbf{F}_c(\mathbf{x}^{(0)}) \right] \quad (4)$$

The particular choice of response correction term originates directly from the correlation analysis presented in Fig. 3. Because the changes of the feature point coordinate are very similar for both the low- and high-fidelity model throughout the design space, the model correction only needs to incorporate the model bias, specifically, the differences between the low- and high-fidelity model characteristic points at a particular design (most conveniently, the centre of the surrogate model domain, i.e.,  $\mathbf{x}^{(0)}$ ). Consequently, the term  $\mathbf{F}_f(\mathbf{x}^{(0)}) - \mathbf{F}_c(\mathbf{x}^{(0)})$  arises naturally. Graphical illustration of the correction mechanism can be found in Fig. 4. As yield estimation is performed by running the MC analysis on the surrogate, its computational cost is only one evaluation of the high-fidelity model and  $2n$  evaluations of the low-fidelity one. For example, if the simulation time ratio between the models is five and  $n = 10$ , the speedup can be as high as 76 percent (the cost of analysis at the level of the surrogate can be neglected).

## 4. Case Study and Results

In this section, the methodology for rapid variable-fidelity-model-based yield estimation is validated using a compact hybrid rat-race coupler, operating at 1 GHz. Several scenarios are considered concerning probability distributions of manufacturing tolerances. Comparison with direct Monte Carlo analysis is also provided.

### 4.1. Miniaturized Rat-Race Coupler

Consider a compact equal-split rat-race coupler (RRC) shown in Fig. 5 [25]. The coupler is implemented on a Rogers RO4003 substrate ( $h = 0.813$  mm,  $\epsilon_r = 3.38$ ). There are eight independent parameters describing the RRC geometry  $\mathbf{x} = [w_1 l_1 l_2 l_3 w_2 l_4 l_5 l_6]^T$ , whereas dimension  $w_0 = 1.7$  is set constant to ensure 50-ohm input impedance. The dependent variables are  $\mathbf{y} = [w_3 w_4]^T$ , where  $w_3 = 20w_1 + 19l_1$  and  $w_4 = 6w_2 + 7l_5$ . All dimensions are in mm. The EM simulation models are implemented in Keysight Momentum: high-fidelity model (5600 mesh cells, simulation time  $\sim 5$  min), low-fidelity model (450 cells,  $\sim 25$  seconds).

### 4.2. Yield Estimation and Benchmarking

The nominal design of the RRC is  $\mathbf{x}^{(0)} = [0.41 \ 0.20 \ 2.19 \ 1.88 \ 0.22 \ 0.43 \ 5.01 \ 7.18]^T$  mm. Design specifications are set to  $dS_{\max} = 0.2$  dB and  $B_{\min} = 100$  MHz.

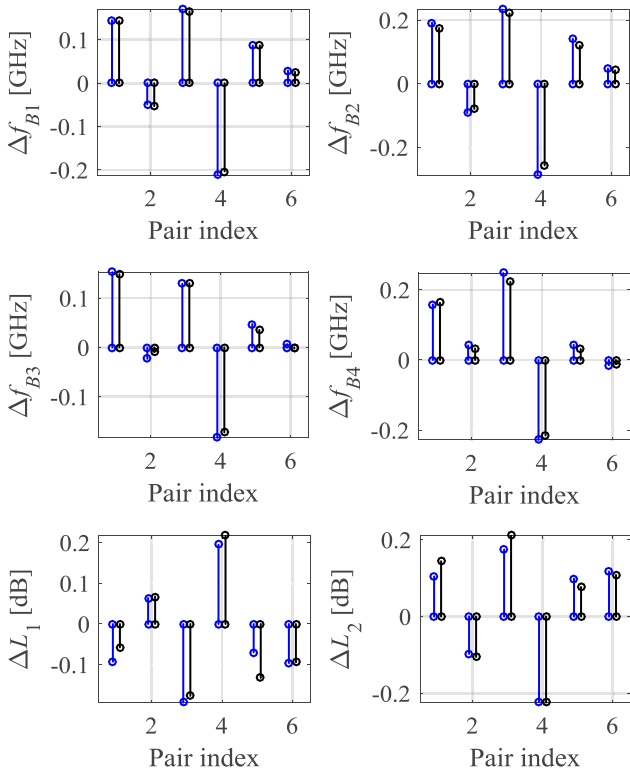


**Fig. 3.** Correlation between response features of the high- (left bars) and low-fidelity model (right bars). Shown are differences between selected feature point coordinates (both frequency and level; for definition see Fig. 1) for several pairs of randomly generated designs.

In order to carry out comprehensive verification, we consider six cases, different in terms of the probability distributions of geometry parameter deviations (all assumed to be independent). Three cases are with uniform distributions and maximum deviations of 0.02 mm, 0.03 mm, and 0.05 mm, respectively. The other three cases are with Gaussian distributions with zero mean and variances of 0.007 mm, 0.01 mm, and 0.017 mm, respectively. The numerical results are gathered in Table 1. Figures 6 and 7 show the RRC comparison of direct EM-based yield estimation and feature-based analysis for the selected cases.

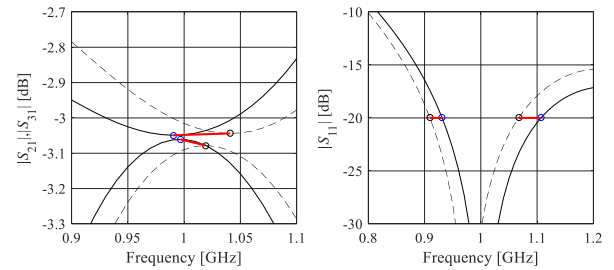


**Fig. 4.** Example responses of the low- (---) and high-fidelity model (—), corresponding feature points (○), as well as feature point correction vectors  $\mathbf{F}_f(\mathbf{x}) - \mathbf{F}_c(\mathbf{x})$  marked using thick lines.

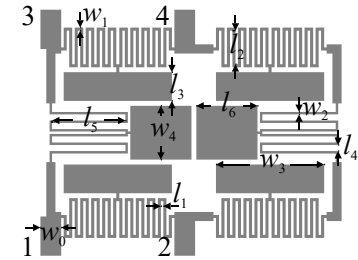


**Fig. 5.** Geometry of the compact microstrip RRC [25].

**Table 1:** Yield Estimation Results for Compact RRC

Case	Design Specs/ Distribution <sup>1</sup>	Yield Estimation Method	Estimated Yield	CPU Cost <sup>2</sup>
I	$dS_{\max} = 0.2$ dB	This work	0.86	2.5
	$B_{\min} = 100$ MHz	High-fidelity FBA <sup>3</sup>	0.87	17
	$U(0.02$ mm)	EM-based MC	0.82	500
II	$dS_{\max} = 0.2$ dB	This work	0.56	2.5
	$B_{\min} = 100$ MHz	High-fidelity FBA <sup>3</sup>	0.56	17
	$U(0.03$ mm)	EM-based MC	0.58	500
III	$dS_{\max} = 0.2$ dB	This work	0.18	2.5
	$B_{\min} = 100$ MHz	High-fidelity FBA <sup>3</sup>	0.20	17
	$U(0.05$ mm)	EM-based MC	0.28	500
IV	$dS_{\max} = 0.2$ dB	This work	0.98	2.5
	$B_{\min} = 100$ MHz	High-fidelity FBA <sup>3</sup>	0.98	17
	$G(0.007$ mm)	EM-based MC	0.96	500
V	$dS_{\max} = 0.2$ dB	This work	0.83	2.5
	$B_{\min} = 100$ MHz	High-fidelity FBA <sup>3</sup>	0.84	17
	$G(0.01$ mm)	EM-based MC	0.81	500
VI	$dS_{\max} = 0.2$ dB	This work <sup>3</sup>	0.59	2.5
	$B_{\min} = 100$ MHz	High-fidelity FBA <sup>3</sup>	0.59	17
	$G(0.017$ mm)	EM-based MC	0.63	500

<sup>1</sup> Probability distribution of parameter deviations:  $U(d)$  – uniform with maximum deviation  $d$ ,  $G(\sigma)$  – Gaussian with zero mean and variance  $\sigma$ .

<sup>2</sup> Estimation cost in number of high-fidelity EM analyses. Feature-based yield estimation utilizes  $N = 5000$  random samples.

<sup>3</sup> FBA – feature-based analysis.

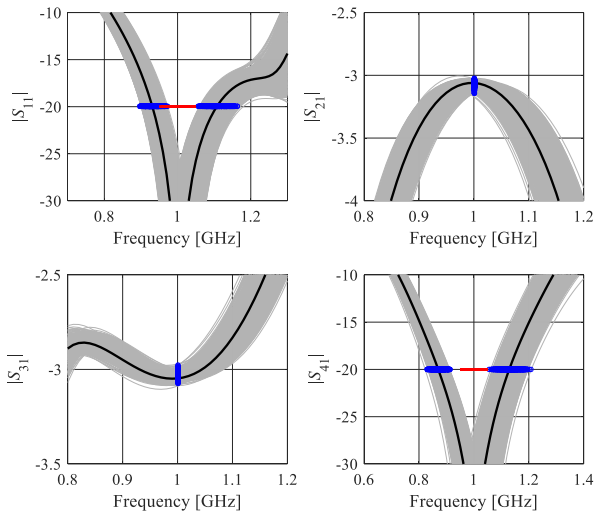


**Fig. 6.** Monte Carlo analysis of the RRC of Fig. 5 using EM simulations (gray plots) and variable-fidelity response feature surrogate model (circles). The nominal design shown black. Shown are plots for Case I of Table 1.

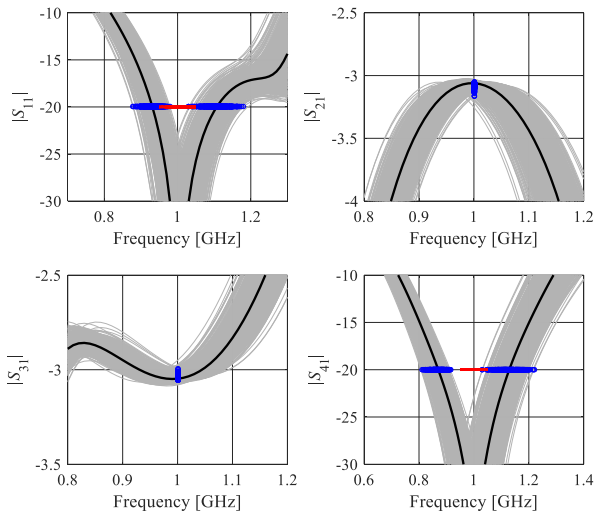


**Fig. 7.** Monte Carlo analysis of the RRC of Fig. 5 using EM simulations (gray plots) and variable-fidelity response feature surrogate model (circles). The nominal design shown black. Shown are plots for Case V of Table 1.

The first observation is that the variable-fidelity response-feature procedure allows for extremely low cost of yield estimation (here, corresponding only to about 2.5 EM simulations of the RRC at high-fidelity level) even though the time evaluation ratio between the high- and low-fidelity model is only around twelve. At the same time, the accuracy of yield estimation using the proposed method (yield estimated using  $N = 5000$  random samples) is very good as confirmed by comparison with direct Monte Carlo analysis ( $N = 500$  samples) and high-fidelity feature-based estimation.

## 5. Conclusion

The paper introduced a technique for rapid yield estimation of miniaturized microwave components. The proposed methodology exploits auxiliary response-feature surrogates constructed using data obtained from low-fidelity

EM simulation model, corrected by means of a single evaluation of the high-fidelity EM model of the coupler. The combination of these two concepts permits yield estimation at extremely low cost of just a few EM analyses (less than three for the considered example of a rat-race coupler). At the same time, the estimation accuracy is very good as confirmed by comparison with two independent methods, direct Monte Carlo analysis and single-level feature-based technique. The topic of the future work will be extension of the proposed technique into a yield-driven design optimization framework.

## Acknowledgments

The authors would like to thank Dassault Systemes, France, for making CST Microwave Studio available. This work was supported in part by the Icelandic Centre for Research (RANNIS) Grant 174114051, and by National Science Centre of Poland Grant 2017/27/B/ST7/00563.

## References

- [1] Y. Zhang, N.K. Nikolova, and M.K. Meshram, "Design optimization of planar structures using self-adjoint sensitivity analysis," *IEEE Trans. Ant. Prop.*, vol. 60, no. 6, pp. 3060-3066, 2012.
- [2] S. Koziel and P. Kurgan, "Inverse modeling for fast design optimization of small-size rat-race couplers incorporating compact cells," *Int. J. RF & Microwave CAE*, vol. 28, no. 5, 2018.
- [3] A. Sheikhi, A. Alipour, and A. Abdipour, "Design of compact wide stopband microstrip low-pass filter using T-shaped resonator," *IEEE Microwave Wireless Comp. Lett.*, vol. 27, no. 2, pp. 111-113, 2017.
- [4] H.L. Ting, S.K. Hsu, and T.L. Wu, "A novel and compact eight-port forward-wave directional coupler with arbitrary coupling level design using four-model control theory," *IEEE Trans. Microw. Theory Techn.*, vol. 65, no. 2, pp. 467-475, 2017.
- [5] A.A. Khan and M.K. Mandal, "Miniaturized substrate integrated waveguide (SIW) power dividers," *IEEE Microwave Wireless Comp. Lett.*, vol. 26, no. 11, pp. 888-890, 2016.
- [6] B. Ma, G. Lei, C. Liu, J. Zhu, and Y. Guo, "Robust tolerance design optimization of a PM claw pole motor with soft magnetic composite cores," *IEEE Trans. Magn.*, vol. 54, no. 3, paper No. 8102404, 2018.
- [7] G. Scotti, P. Tommasino, and A. Trifiletti, "MMIC yield optimization by design centering and off-chip controllers," *IET Proceedings - Circuits, Devices and Systems*, vol. 152, no. 1, pp. 54-60, Feb. 2005.
- [8] A. Kouassi, N. Nguyen-Trong, T. Kaufmann, S. Lallechere, P. Bonnet, and C. Fumeaux, "Reliability-aware optimization of a wideband antenna," *IEEE Trans. Ant. Prop.*, vol. 64, no. 2, pp. 450-460, 2016.
- [9] Z. Ren, S. He, D. Zhang, Y. Zhang, and C.S. Koh, "A possibility-based robust optimal design algorithm in preliminary design state of electromagnetic devices," *IEEE Trans. Magn.*, vol. 52, no. 3, paper No. 7001504, 2016.
- [10] A.S.O. Hassan, H.L. Abdel-Malek, A.S.A. Mohamed, T.M. Abulfadl, and A.E. Elqenawy, "Statistical design centering of RF cavity linear accelerator via non-derivative trust region optimization," *IEEE Int. Conf. Numerical Electromagnetics Multiphysics Mod. Opt. (NEMO)*, pp. 1-3, 2015.
- [11] R. Biernacki, S. Chen, G. Estep, J. Rousset, J. Sifri, "Statistical analysis and yield optimization in practical RF and microwave systems," *IEEE MTT-S Int. Microw. Symp. Dig.*, Montreal, pp. 1-3, Jun. 2012.
- [12] I. Syrytsin, S. Zhang, G.F. Pedersen, K. Zhao, T. Bolin, and Z. Ying, "Statistical investigation of the user effects on mobile

terminal antennas for 5G applications,” *IEEE Trans. Ant. Prop.*, vol. 65, no. 12, pp. 6596-6605, 2017.

- [13] P. Manfredi and F. G. Canavaro, “Efficient statistical simulation of microwave devices via stochastic testing-based circuit equivalents of nonlinear components,” *IEEE Trans. Microwave Theory Techn.*, vol. 63, no. 5, pp. 1502-1511, 2015.
- [14] J. Du and C. Roblin, “Statistical modeling of disturbed antennas based on the polynomial chaos expansion,” *IEEE Ant. Wireless Prop. Lett.*, vol. 16, p. 1843-1847, 2017.
- [15] M. Rossi, A. Dierck, H. Rogier, and D. Vande Ginste, “A stochastic framework for the variability analysis of textile antennas,” *IEEE Trans. Ant. Prop.*, vol. 62, no. 16, pp. 6510-6514, 2014.
- [16] M. Sengupta, S. Saxena, L. Daldoss, G. Kramer, S. Minehane, and J. Cheng, “Application-specific worst case corners using response surfaces and statistical models,” *IEEE Trans. Comput.-Aided Design Integr. Circuits Syst.*, vol. 24, no. 9, pp. 1372-1380, Sep. 2005.
- [17] E. Matoglu, N. Pham, D. De Araujo, M. Cases, and M. Swaminathan, “Statistical signal integrity analysis and diagnosis methodology for high-speed systems,” *IEEE Trans. Adv. Packaging*, vol. 27, no. 4, pp. 611-629, Nov. 2004.
- [18] J. Zhang, C. Zhang, F. Feng, W. Zhang, J. Ma, and Q.J. Zhang, “Polynomial chaos-based approach to yield-driven EM optimization,” *IEEE Trans. Microwave Theory Tech.*, vol. 66, no. 7, pp. 3186-3199, 2018.
- [19] J.S. Ochoa, and A.C. Cangellaris, “Random-space dimensionality reduction for expedient yield estimation of passive microwave structures,” *IEEE Trans. Microwave Theory Techn.*, vol. 61, no. 12, pp. 4313-4321, Dec. 2013.
- [20] S. Koziel, J. Bandler, A. Mohamed, and K. Madsen, “Enhanced surrogate models for statistical design exploiting space mapping technology,” in *IEEE MTT-S Int. Microw. Symp. Dig.*, Long Beach, CA, pp. 1-4, Jun. 2005.
- [21] H.L. Abdel-Malek, A.S.O. Hassan, E.A. Soliman, S.A. Dakrouy, “The ellipsoidal technique for design centering of microwave circuits exploiting space-mapping interpolating surrogates,” *IEEE Trans. Microwave Theory Techn.*, vol. 54, no. 10, pp. 3731-3738, Oct. 2006.
- [22] S. Koziel and J.W. Bandler, “Rapid yield estimation and optimization of microwave structures exploiting feature-based statistical analysis,” *IEEE Trans. Microwave Theory Tech.*, vol. 63, no., 1, pp. 107-114, 2015.
- [23] S. Koziel, “Fast simulation-driven antenna design using response-feature surrogates,” *Int. J. RF & Microwave CAE*, vol. 25, no. 5, pp. 394-402, 2015.
- [24] Q.S. Cheng, S. Koziel, and J.W. Bandler, “Simplified space mapping approach to enhancement of microwave device models,” *Int. J. RF and Microwave Computer-Aided Eng.*, vol. 16, no. 5, pp. 518-535, 2006.
- [25] S. Koziel, and A. Bekasiewicz, “Expedited geometry scaling of compact microwave passives by means of inverse surrogate modeling,” *IEEE Trans. Microwave Theory Tech.*, vol. 63, no. 12, pp. 4019-4026, 2015.

